SAND2021-8694C

Proceedings of the INMM & ESARDA Joint Virtual Annual Meeting
August 23-26 & August 30-September 1, 2021

Magnetic **S**mart **T**ag (**MaST**) for Unique Identification

Eric Langlois
MEMS Technologies
Sandia National Laboratories
Albuquerque, NM, 87185, USA
elanglo@sandia.gov

Jamin Pillars
Multiscale Fab Sci & Tech Dev
Sandia National Laboratories
Albuquerque, NM, 87185, USA
jrpilla@sandia.gov

Todd Monson
Nanoscale Sciences
Sandia National Laboratories
Albuquerque, NM, 87185, USA
tmonson@sandia.gov

Patrick Finnegan
MEMS Technologies
Sandia National Laboratories
Albuquerque, NM, 87185, USA
psfinne@sandia.gov

Barny Doyle
Radiation-Solid Interactions
Sandia National Laboratories
Albuquerque, NM, 87185, USA
bldoyle@sandia.gov

LaRico Treadwell
Advanced Materials Laboratory
Sandia National Laboratories
Albuquerque, NM, 87185, USA
ljtread@sandia.gov

Heidi Smartt
Intl Safeguards & Engagements
Sandia National Laboratories
Albuquerque, NM, 87185, USA
hasmart@sandia.gov

Nicholas Gurule
Renewable, Distributed Sys Int
Sandia National Laboratories
Albuquerque, NM, 87185, USA
nsgurul@sandia.gov

Charles Pearce
Nanoscale Sciences
Sandia National Laboratories
Albuquerque, NM, 87185, USA
cjpearc@sandia.gov

Benjamin Lehman
MEMS Technologies
Sandia National Laboratories
Albuquerque, NM, 87185, USA
bilehma@sandia.gov

Abstract

High value assets, including containers of nuclear material, often require unique identifiers (UIDs) to mitigate the issue of counterfeit or substitution as well as facilitating inventory. These UIDs should be: 1) extremely difficult to counterfeit; 2) robust to environmental conditions; 3) safe and secure for facility and personnel; 4) low maintenance; and 5) easily verified without the use of image comparison techniques. Problems surrounding existing identification include a lack of uniqueness and swift (i.e., electronic) interrogation, making verification difficult, time consuming, and labor intensive. We have developed a new, wireless, Magnetic Smart Tag (MaST) technology for uniquely identifying nuclear materials and other high value assets. MaST is comprised of passive, magnetic alloy resonator arrays vibrating at multiple resonant frequencies when excited with low frequency alternating current (AC) magnetic fields creating a unique, nonreproducible, complex signature. The identity of a MaST, including its authenticity and integrity, can be verified in situ by a near field magnetic reader. Unlike radio frequency tags, MaST operates magnetically at low, operationally safe strengths. This UID, due to its small size, i.e., centimeters to inches, can be unobtrusively attached to the walls of new and existing nuclear fuel containers and equipment. MaST is wireless, passive, i.e., no batteries required, stable, and robust, thus providing a long service life. MaST signatures depend on resonator geometry rather than electronic memory enabling its survival in radiation environments. MaST will be targeted towards applications of interest such as spent fuel rod storage and radiological sources such as those employed for medical diagnostics and well logging.

Keywords: Tagging, magnetic, magnetostrictive, NiFeCo

I. Introduction

A. Mission Problem

High value assets, including containers of nuclear material, often require unique identifiers (UIDs) to mitigate the issue of counterfeit or substitution as well as facilitating inventory. These UIDs should be: 1) extremely difficult to counterfeit; 2) robust to environmental conditions; 3) safe and secure for facility and personnel; 4) low maintenance; and 5) easily verified without the use of image comparison techniques. Problems surrounding existing identification include a lack of uniqueness and swift (i.e., electronic) interrogation, making verification difficult, time consuming, and labor intensive. Radiological materials in need of UIDs include UF6 containers [1], highly radioactive Co-60 or Cs-137 sources, radioactive isotopes used for medical diagnostics or treatment (e.g., Gamma Knife) [2], AmBe neutron sources for well logging [3], nuclear weapon containers and transportation vehicles [4], etc. (Fig. 1).

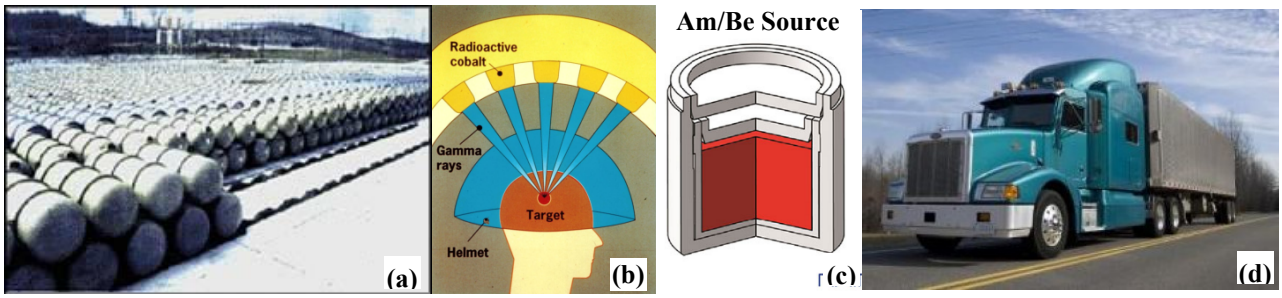

Figure 1.(a) UF6 cylinders, (b) Gamma Knife cobalt sources, (c) AmBe neutron source, (d) ND transportation trucks.

B. Current State of the Art/Practice

Intrinsic features and applied tags are two approaches to identification. Intrinsic features recorded using near-field imagery (e.g., laser scanning, ultrasonic imaging) have been studied. Tagging has been explored using optical barcodes, **r**eflective **p**article **t**ags (**RPT**s), and radio-frequency identifiers (RFIDs), yet these too have had issues in practical application. Barcodes are easily duplicated or spoofed. RPTs [5] are extremely difficult-to-counterfeit but rely on image comparison for verification as well as direct contact with the tagged surface (Fig. 2). Operators resist the use of RFIDs in their facilities for both safety reasons (e.g., risk of explosives activation, interference with medical pacemakers) and communications interference. Additionally, barcodes may be vulnerable to accidental damage or malicious tamper and RFIDs may suffer from detuning due to proximity to metallic objects.

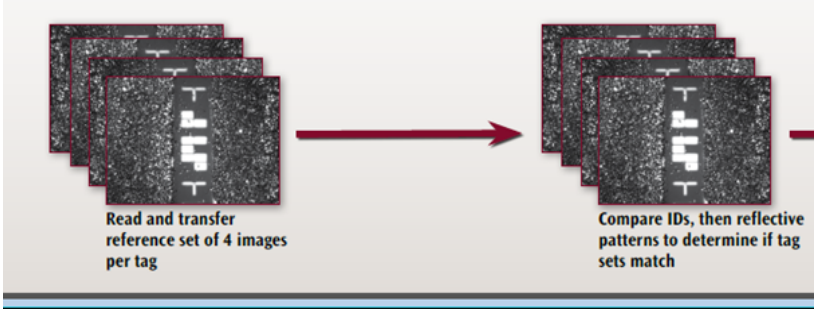

Figure 2. An RPT reader images the RPT tag from multiple lighting angles and compares the reflections for verification.

C. MaST

Our solution to solve this mission need is a novel, Sandia-developed technology called a magnetic smart tag (MaST). MaST exploits the physical properties of magnetostriction (an induced microstrain in response to an external applied magnetic field), a characteristic of certain ferromagnetic alloys such as nickel-iron-cobalt (NiFeCo). Each MaST would exhibit a unique multiple-frequency/multiple-amplitude signature associated with a microfabricated array of resonant NiFeCo structures using a first-of-its-kind Sandia developed electrodeposition process. Different resonator lengths provide different resonant frequencies (Fig. 3) while multiple, same frequency resonators provide different resonant amplitudes. Anti-counterfeit properties making this technology nearly impossible to replicate include the following: 1. Proprietary NiFeCo alloy electroplating, 2. Multi-bit arrays, 3. Unique array patterning, and 4. Post-processing randomness (e.g., randomly patterned thin film coatings). MaST, due to its small size, e.g., centimeters to inches, and radiation hardness can be attached to the various high value, radiological assets mentioned previously.

This paper provides an overview of the status and challenges of MaST. The theory of operation is described in Section I, covering magnetomechanical resonance theory, the bench top characterization setup, and method of interrogation. Section II covers unique design aspects of MaST including resonator anchoring and the use of random resonator arrays that form it's UID. Section IV goes over Sandia's novel magnetostrictive NiFeCo electroforming microfabrication technology for building a MaST while Section V describes the various environmental testing MaST has undergone thus far, including elevated temperature and radiation testing, providing evidence of feasibility for field deployment. Conclusions are finally given in Section VI.

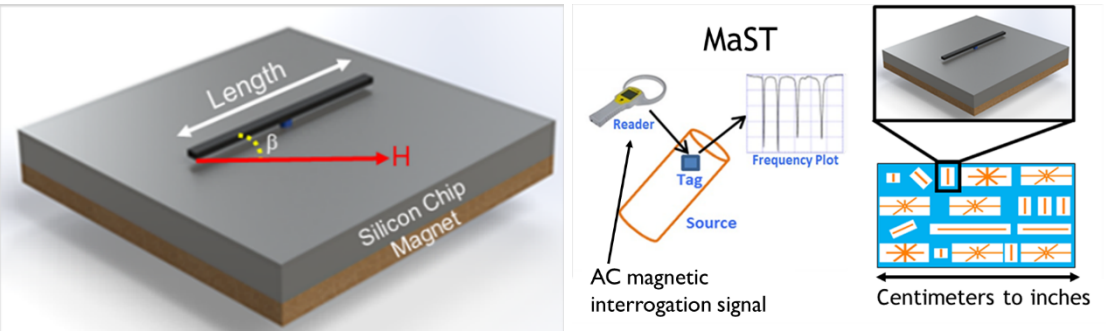

Figure 3. (left) Resonator architecture with permanent magnet. (right) Simplified MaST concept.

II. Theory of Operation

A. Magnetomechanical Resonance

In passive radio-frequency identification (RFID) systems, the reader transmits a modulated RF signal to the tag consisting of an antenna and an integrated circuit chip forming a resistance, inductance, and capacitance (RLC) circuit. The chip receives power from the antenna and responds by varying its input impedance and thus modulating the backscattered signal. In contrast to the modulated, single carrier frequency of these well-established RFID systems, the MaST signature is based upon a multiple-frequency/variable-amplitude spectral signature that is unique to every MaST. This signature is the result of a random pattern of microns thin, rectangular, magnetostrictive NiFeCo alloy longitudinal-mode resonators. Longitudinal-mode resonators vibrate through cycles

of in-plane expansion and contraction along their length. The magnetomechanical longitudinal-mode vibration in our NiFeCo resonators occurs through a property called Joule magnetostriction where an oscillating mechanical micro-strain is induced by an **a**lternating **c**urrent (**AC**) magnetic interrogation field. A biasing magnetic field is supplied by a thin sheet of hard magnetic material, which holds the resonator near its optimum magnetoelastic coupling point where the modes are strongest. If a periodic magnetic signal is imposed by a drive antenna, the resonator will undergo mechanical oscillation that is maximized at its magnetomechanical resonance frequency defined by equation 1 [6]:

$$f_r = \frac{1}{2L}\left[\sqrt{\frac{\rho}{E_0} + \frac{9\lambda_s^2\rho\left(\left(|H_B|\cos(\beta)\right)\right)^2}{J_s H_A^3}}\right]^{-1}, \quad (1)$$

where L is the strip length, ρ is the material density, E_0 is the Young's modulus at zero field, λ_S is the saturation magnetostriction, H_B is the magnetic bias field, β is the angle between the resonator main axis and H_B, J_S is the saturation polarization, and H_A is the shape anisotropy field, i.e., the field required to rotate the magnetic domains to align along the hard axis direction. To first order, the resonance frequency is determined by the length, L, and the bias angle, β.

B. Bench Top Setup

Laboratory-level MaST interrogation is accomplished presently using a **v**ector **n**etwork **a**nalyzer (**VNA)**, a set of Helmholtz coils, and a **p**rinted **c**ircuit **b**oard (**PCB**) loop antenna. The type of planar loop antenna used is called a butterfly or figure 8 coil. This coil is ideally suited for bench top characterization of these resonators as it can produce a strong magnetic flux density with flux lines oriented parallel to its surface at the center while being energized with low input current values such as those outputted by the VNA. This allows either a single resonator or an entire MaST to be energized with an AC magnetic field that is preferentially aligned parallel to the long or easy axis of the resonator for maximum signal intensity near the coil surface. It also fits well within the uniform magnetic field region of the Helmholtz coil pair, providing a biasing field that can be varied using an external DC power supply (not shown). The input and output ports of the PCB loop antenna are connected to the respective connections on the VNA. Finally, a 3-D printed fixture is used to spatially fix in place both the PCB loop antenna and the MaST, with respect to each other, to minimize run-to-run measurement errors due to distance and angular variability. While not ideally suited for field deployment, where a more portable, hand-held interrogator is needed, nevertheless, this setup is very flexible for providing bench top characterization data, particularly during the development stages of our NiFeCo resonators where materials properties are changing and continuing to improve.

C. Interrogation

The measurement begins by inputting a signal from the VNA that is swept across a frequency range where the expected fundamental resonance of a single resonator or resonators is expected to occur according to Eqn. 1. The S_{11} or reflection parameter of the loop antenna is monitored during this sweep. The oscillating magnetic field of the loop antenna sets up a corresponding mechanical vibration in the resonator achieving a maximum value at resonance. Since magnetostriction is primarily an energy absorption process, this manifests as a frequency notch in the S_{11} signal

spectrum. During each sweep, the Helmholtz coils are slowly energized while watching the fundamental notch grow in intensity. A maximum absorption signal is reached when the applied magnetic field, $H_{APPLIED}$, is equal to the anisotropy field, H_A, and increasing or decreasing $H_{APPLIED}$ only reduces the intensity of the signal notch. This absorption signal is shown in the VNA screen in Fig. 4.

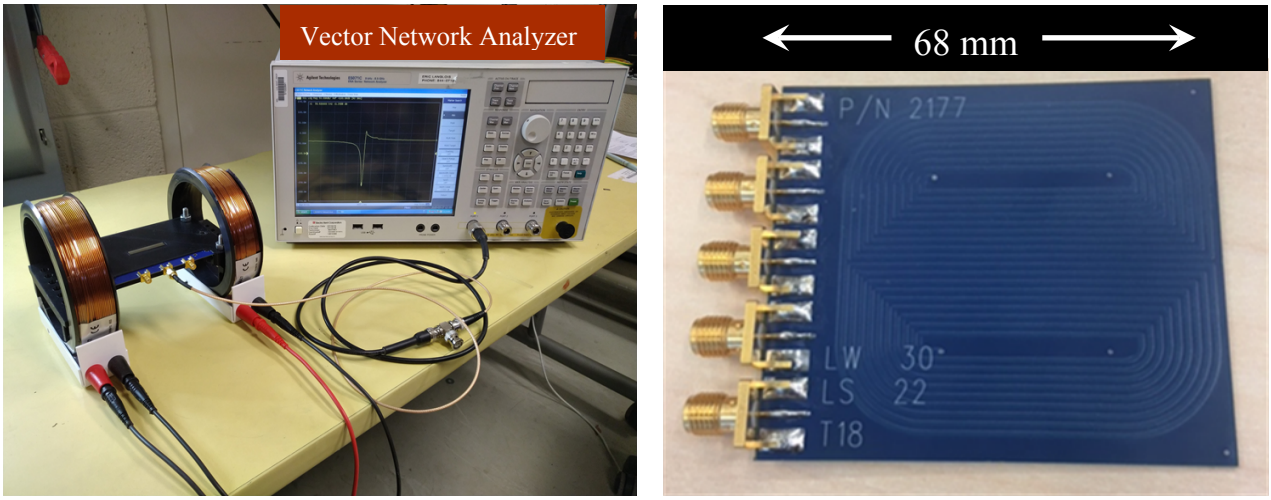

Figure 4. (left) MaST benchtop interrogation setup comprised of a VNA, a pair of Helmholtz coils, a PCB loop antenna, a 3-D printed resonator fixture, cabling, and connectors. (right) A close-up image of the PCB loop antenna.

III. Design

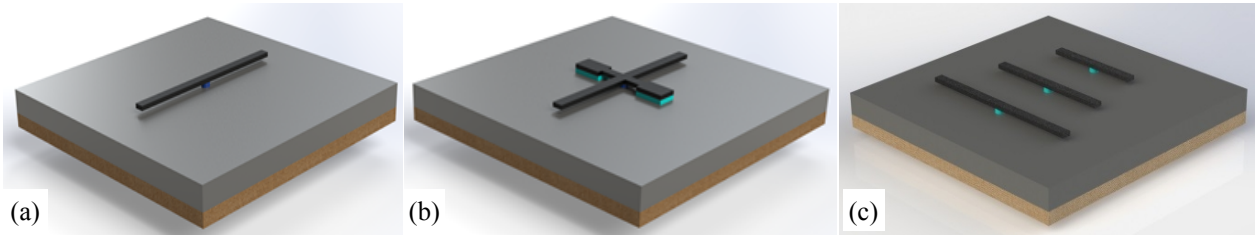

Figure 5. (a) Single frequency resonator supported by a central post. (b) Single frequency resonator supported by side tethers and anchor posts. (c) Multifrequency resonator array (three distinct resonance frequencies).

A. Resonator Anchoring

An illustration of one of these resonators, shown on the left in Fig. 5, is of a rectangular bar of NiFeCo alloy, freely suspended along most of its length except for a central post anchoring it to a substrate. This anchoring scheme allows the resonator to vibrate freely, without suffering damping effects induced by substrate surface friction, while remaining attached to the substrate surface. The choice of substrate shown in Fig. 3 is silicon, but it can be comprised of any highly resistive material, e.g., glass, sapphire, plastic, as it primarily serves as a mechanical foundation and nothing more, as no on-board electronic circuitry is required. The need for high resistivity is to avoid magnetic eddy current losses in the substrate that will reduce signal power and interfere with signal transmission. Similarly, while the position of the central post is important as it is a mechanical null point, the choice of anchor material can be variable, e.g., NiFeCo, silicon nitride, or any other low-

cost, microfabrication-compatible material. There are couple of options when it comes to the choice of anchor architecture. Fig. 5 (a) shows a single anchor post situated directly underneath the resonator, suspending it above the substrate. One can also support the resonator through a set of two anchor posts that are attached by a pair of thin, co-planar NiFeCo support tethers that extend sideways from the resonator center (Fig. 5 (b)). Fig. 5 (c) shows a small array of three resonators with different lengths and, thus, three different resonance frequencies.

B. Identification

The inherent design flexibility of MaST can enable millions of unique signature combinations. This can be shown numerically by the following combinatorial equation 2 [6]:

$$\boldsymbol{N_K = \frac{N_T!(N_W - 1)!}{2N_R!(N_T - N_R)!(N_W - N_R)!}} \quad , \tag{2}$$

where N_T is the number of resonator types, N_R is the number of resonators present, N_W is the number of possible angles, making N_K the number of coded tags possible. For example, $N_T = 5$, $N_R = 12$, $N_W = 18$ gives a total of 22,619,520 different possible codes for N_K. This is only accounting for variation in frequency space and not even taking into consideration the possible variation in amplitude space. Since resonance amplitude varies with the number of resonators of the same fundamental frequency, variable resonance amplitude also contributes to the MaST identity. Thus, MaST footprints can range anywhere from centimeters to inches and be less than millimeters in thickness allowing the tag to be unobtrusive or placed in areas in which larger tags may not fit. Ultimately, the code complexity, i.e., the number of code combinations, remains a matter of debate to be settled by end-users in those targeted application spaces.

Methods for remotely interrogating magnetostrictive resonators have been explored by researchers doing similar work by hand assembling resonators cut from commercial magnetic alloy ribbon [6-8]. However, the inability to manufacture using batch fabrication techniques and the relatively large tag sizes mentioned makes these approaches cost prohibitive, limiting their overall usefulness.

IV. Microfabrication

A. Electroforming Advantages

Our novel approach is to electroform magnetostrictive NiFeCo alloy-based resonators. Electrodeposition is an ideal batch fabrication technology for depositing metal alloy layers with the necessary stoichiometry, material properties, and low stress needed with a high degree of constituent material control. Electrodeposition is performed in a chemical bath with a seed metal coated substrate forming a cathode and some sort of metal plate or mesh forming an anode. The reduction of metal cations on to the seed metal coated substrate occurs by means of electric current provided by an external power supply. When combined with photolithographically patterned resist molds (i.e., electroforming), thick, patterned, resonators with different lengths are possible to create multifrequency arrays of magnetic resonators constituting the identity of the MaST.

B. Electrodeposition of High Magnetostriction NiFeCo Alloy

An acidic chemistry was developed for the electrodeposition of NiFeCo to control the ratio of Ni:Fe:Co and allow for the addition of small atomic percentages of other elements to adjust the mechanical, electrical, or magnetic properties of the alloy. The concentrations of Ni, Fe, and Co in the chemistry must be carefully controlled to have the proper ratio in the deposited film. Iron group metals will catalyze the deposition of other metals, including other iron group elements. This means that nickel will "help" or lower the energy required to deposit cobalt and that their starting concentrations in the chemistry are not reflected in the concentrations in the deposited film. This phenomenon is called anomalous co-deposition and occurs between the Ni, Fe, and Co in this system. This ratio is critical to the function of the alloy material as too high a concentration of Co or Fe and the material will not produce a resonant response.

After electrodeposition, the alloy material is placed in a tube furnace with inert nitrogen flowing for an annealing process. The inert environment limits any oxidation of the material during the annealing step. While a small resonance response is measurable with unannealed material, the annealing step increases the signal amplitude by orders of magnitude. The anneal accomplishes this through re-shaping the B-H curve, tilting it away from a square shape [9], and by releasing hydrogen and water trapped in the material during the electrodeposition process. Fig. 6 provides a comparison of the S_{11} resonance signal between NiFeCo and commercial USIII Metglas ribbon.

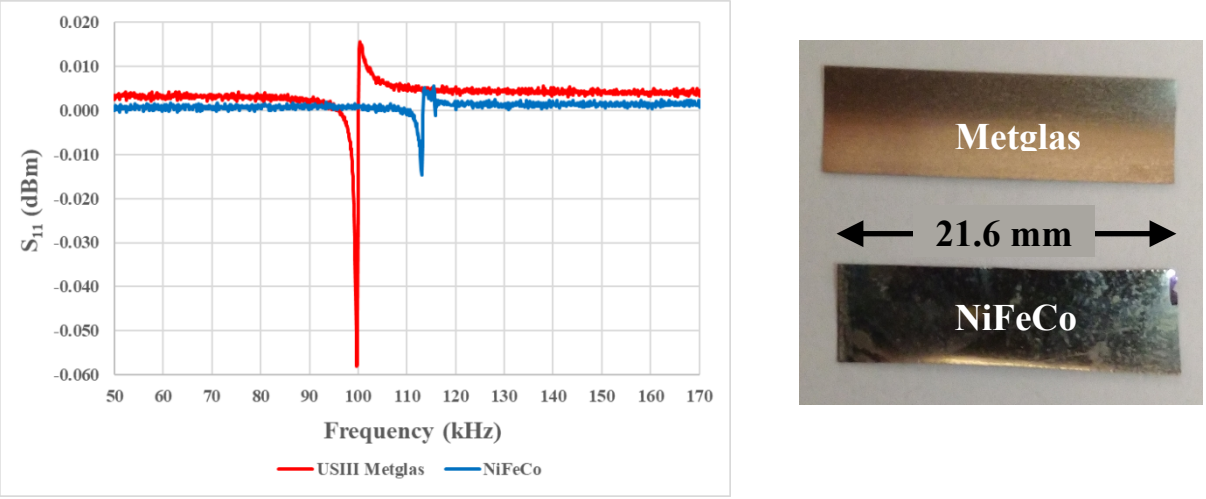

Figure 6. (left) S_{11} measurement comparing USIII Metglas vs. electrodeposited NiFeCo resonators. (right) Side-by-side image comparison of the two resonators.

C. Resonator Process Integration

To fabricate arrays of resonators to form a MaST, a microfabrication process flow must be developed. Two fabrication approaches are being explored as a two-tiered risk mitigation approach. One uses a Polymethylglutarimide (PMGI) sacrificial layer and the other a silicon sacrificial layer. A sacrificial layer is the material layer directly underneath the NiFeCo resonator that gets preferentially etched away during the final process step, releasing the resonator. PMGI, a deep UV photo definable polymer, can be put down with coating thicknesses ranging from 1 µm to 5 µm and is unique in that it can pattern a second photoresist on top due to its resistance to most conventional solvents, developers and temperature. The PMGI sacrificial layer can be removed by specific

solvents that will not affect the NiFeCo or the surrounding substrate. Using silicon as a sacrificial layer has many similarities in processing but enables a potentially more stable, xenon difluoride

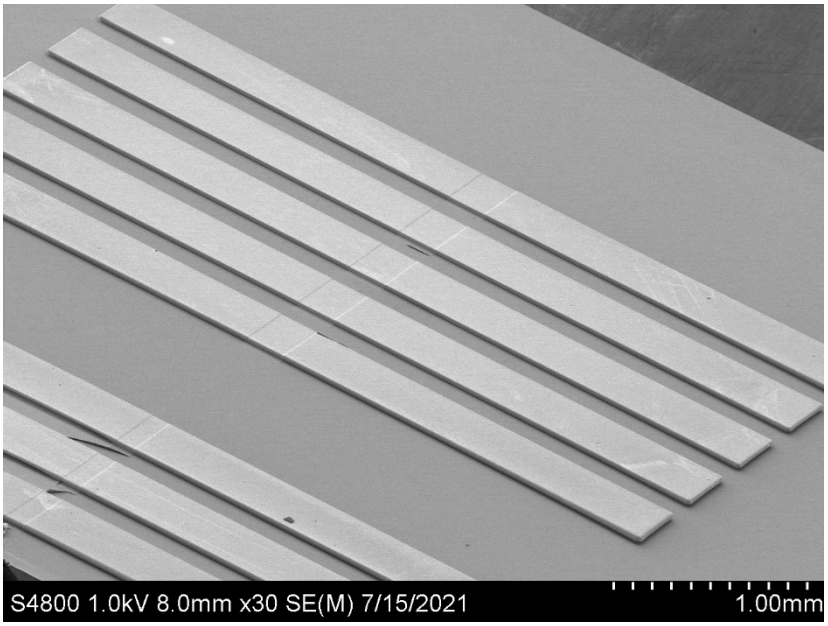

Figure 7. Scanning electron micrograph (SEM) image of a NiFeCo resonator array.

(XeF2) dry etch release that will also not affect the NiFeCo resonator. Both fabrication approaches should result in a fully formed resonator arrays that are anchored to the substrate (Fig. 7). Currently, difficulties regarding seed metal integrity during etch release are being encountered. Once these get resolved, microfabricating functioning MaSTs should be possible.

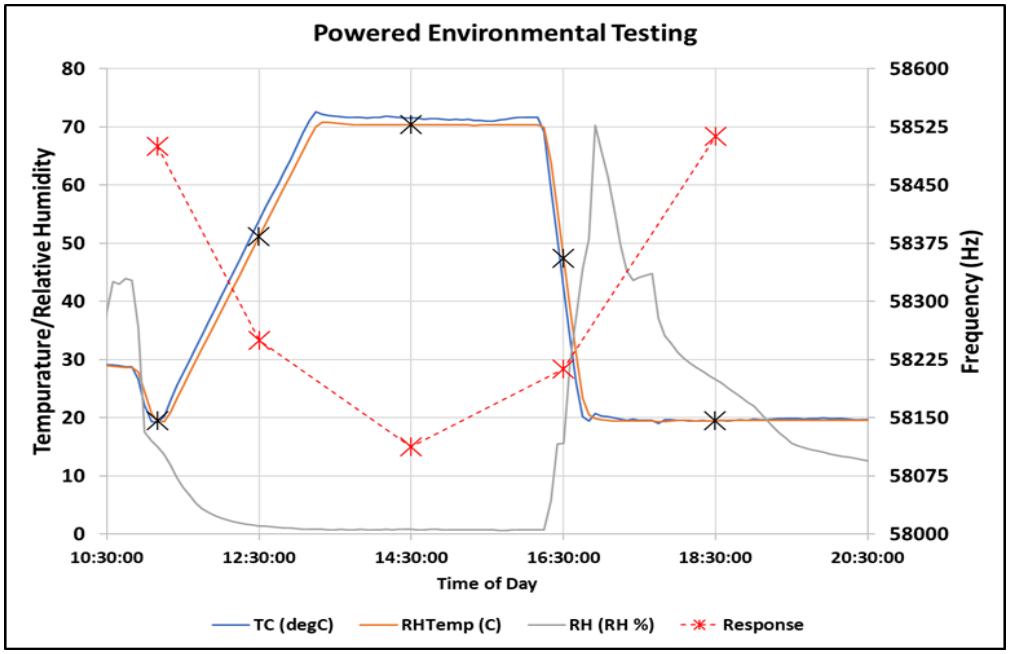

Figure 8. Environmental testing profile and frequency measurement for an operational USIII Metglas resonator.

V. Environmental Testing

A. Temperature and Humidity Testing

One of the outstanding questions regarding the long-term operational performance of MaST is how the frequency signature is affected by variable temperature and humidity. Given that we didn't have working NiFeCo resonators at the time of the test, we substituted commercial USIII Metglas resonators, with similar magnetomechanical behavior and elemental stoichiometry, as a proxy. Two USIII resonators were tested under electrical interrogation during a single cycle test. During the test, the temperature was cycled between room temperature and 70 °C and the relative humidity was cycled between 0% and 70% (Fig. 8). Over the course of the 10-hour test, the two resonators experienced a less than 400 Hz shift in resonance frequency. This is good news from the standpoint of how minor a shift it is in relation to the fundamental peak frequency and that this minor shift could be eliminated altogether through the application of an appropriately sized bias magnetic field. As explained at the beginning of the project, these magnetic alloys have a magnetic dependent coefficient of Young's modulus that can be used to cancel out their temperature dependence, thus making their resonance frequency stable over a wide temperature range. From early literature regarding commercial magnetoelastic resonators, we know it is possible to either cancel out or enhance temperature effects on resonator frequency shifts through the appropriate application of certain bias magnetic fields [10]. This is possible due to the unique interaction between the applied magnetic field and the thermomagnetic component of Young's modulus.

To determine the effect of elevated temperature on the resonant frequency, a commercial US III resonator was subjected to a temperature range of 20-60°C with a varying dc bias field to replicate these results. From this test it was determined that, with a magnetic field bias around 320 A/m, close to the natural peak response, the resonator has the least amount of temperature dependency (Fig. 9). The plan is to repeat this test using NiFeCo resonators to see if the same temperature cancellation property is present.

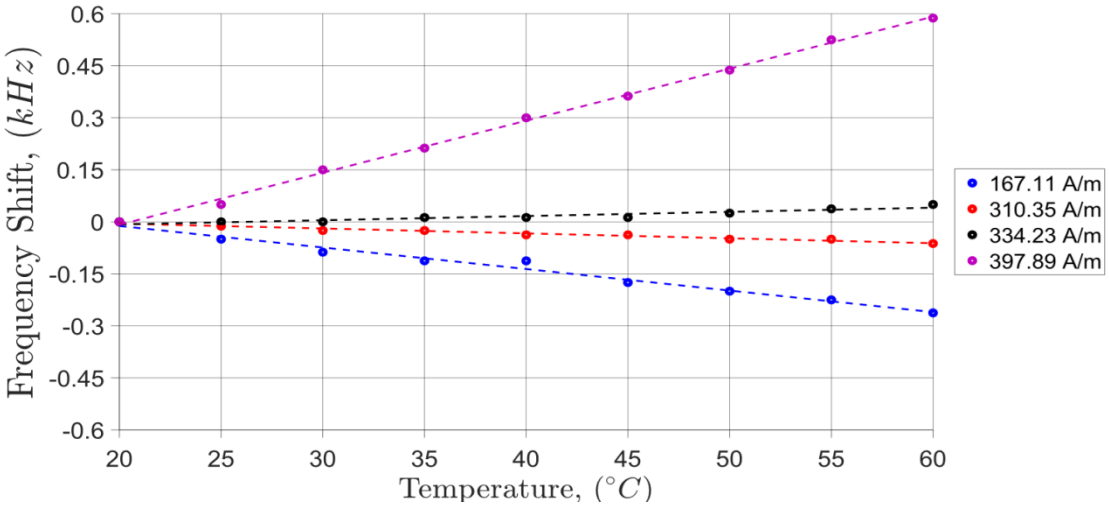

Figure 9. Plot of frequency shift as a function of magnetic bias field and temperature.

B. Radiation Testing

Due to the decades-long operational lifetimes the MaST is expected to survive under constant exposure to ambient radiation, accelerated testing using a Pelletron MeV proton accelerator at the **I**on **B**eam **L**aboratory (**IBL**) at Sandia seemed an ideal solution for this task. Prior to testing,

identification of what the ranges are for the various types of radiation encountered is important. According to the **I**nternational **A**tomic **E**nergy **A**gency (**IAEA**) Qualification Test Procedures SG-OP-GNRL-TP-0001 document, the range of both gamma and neutron dose rates expected for spent fuel rods, SNM, and radioactive sources used for medical applications would fall under category "A" radioactive direct use materials. These ranges are the following:

1. Gamma radiation: .01-20 Gy/hr, or a maximum of 1.75e9 rads/century
2. Thermal neutrons: 10^4-10^8 n/cm^2/s (we can't simulate thermal neutrons in the IBL)
3. Fast Neutrons 10^3-10^7 n/cm^2/s, or a maximum of 3.15e16 n/cm^2/century

The choice of 2.8 MeV protons was arrived at for two reasons: 1. This energy is adequate to penetrate the entire 25 um thickness of the resonators, and 2. is achievable by the Pelletron accelerator. After making this selection we calculated the dose rate and equivalent 1 MeV energy neutron fluxes achievable with these protons over the entire resonator. This was done using the famous Ziegler, Biersack and Littmark theory for electronic and nuclear stopping power [11]. These stopping powers were then converted to ionizing and non-ionizing radiation production rates in unit of rads/s and 1 MeV equivalent n/cm^2/s. It was found that protons with a fluence of 10^{15} p/cm^2 provide a century level gamma-equivalent dose rate slightly less than the IAEA procedure, and a neutron fluence slightly greater. This is summarized in the Table 1 with a plot of the comparison shown in Fig. 9. Pre-and-post measurements of an electroplated NiFeCo resonator exposed to a 100-year lifetime radiation dose is shown in Fig. 10. Do discernible shift in resonance frequency or reduction in signal amplitude is observed proving operational lifetime radiation hardness.

Table 1. Summary of IAEA specified gamma dose rate and neutron fluences compared to simulated proton fluences.

	Rads/century	n/cm^2/century
IAEA Test	1.75x10^9	3.15x10^{16}
2.8 MeV Proton Exposure	1.38x10^9	4.16x10^{16}

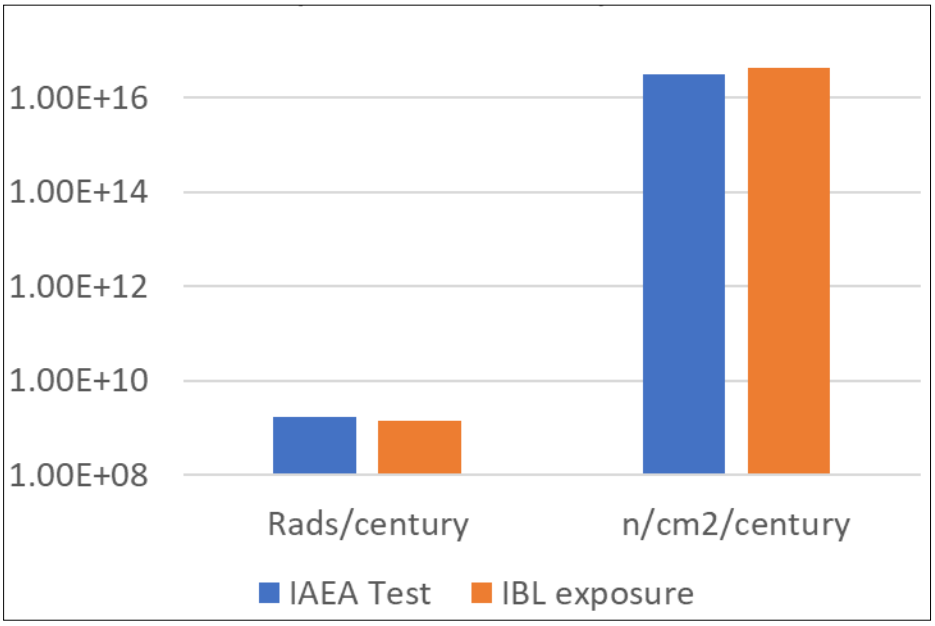

Figure 10. Comparison of Pelletron 2.8 MeV proton resonator exposures to IAEA qualification test.

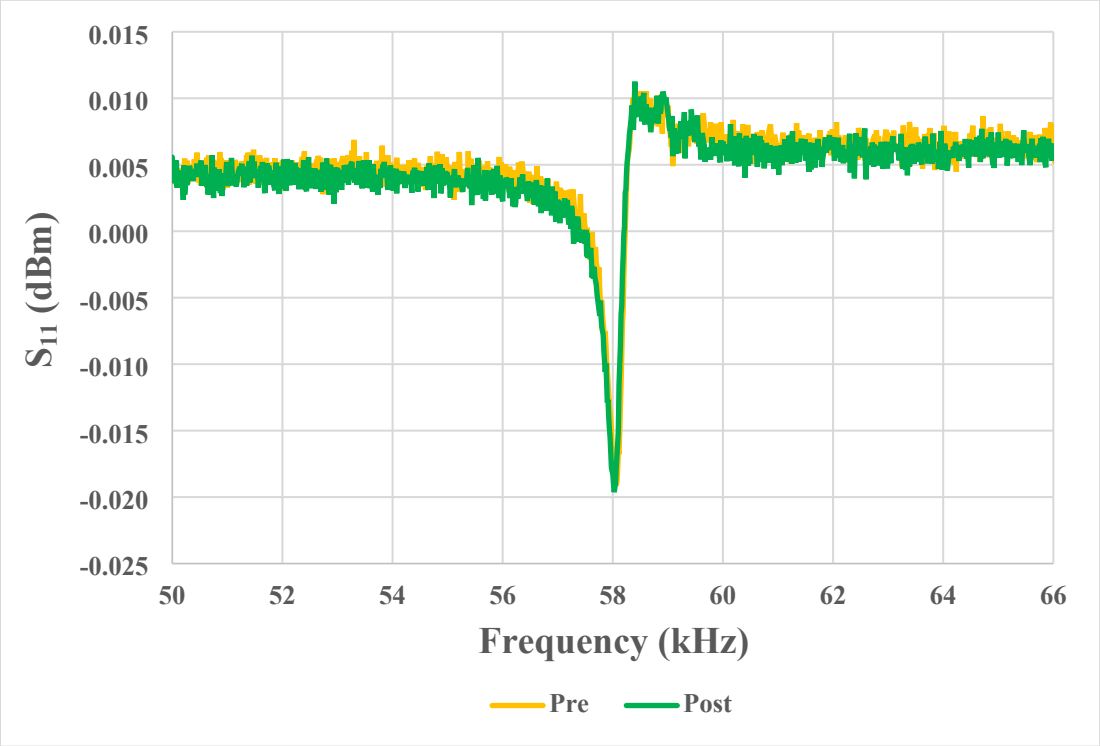

Figure 11. Pre-and-post measurement of NiFeCo resonator exposed to accelerated 100-year radiation exposure. No discernible frequency shift observed proving operational lifetime radiation hardness.

VI. Conclusions

A novel magnetic smart tag, or MaST, is described in this paper. The identity of a MaST, including its authenticity and integrity, can be verified in situ by a near field magnetic reader at low, operationally safe strengths. This UID, due to its small size, i.e., centimeters to inches, can be unobtrusively attached to the walls of new and existing nuclear fuel containers and equipment. MaST is wireless, passive, i.e., no batteries required, stable, and robust, thus providing a long service life. MaST signatures depend on resonator geometry rather than electronic memory enabling its survival in high radiation environments. MaST is enabled by a novel, magnetostrictive electroforming technology developed at Sandia. This new microfabrication process can create massively parallel resonator arrays providing unique multiple-frequency/variable-amplitude signatures for each MaST. Due to the unique properties of magnetostrictive materials, temperature-induced frequency shifts can be cancelled out providing stable tag performance across a wide temperature range. Finally, MaST has a demonstrated radiation hardness and can be field deployed for 100 years and, perhaps, even longer.

VII. Acknowledgments

This project was supported by the National Nuclear Security Administration, Defense Nuclear Nonproliferation Research and Development (NA-22), project number SL19-Magnetic Smart Tag (MAST)-PD1La. Sandia National Laboratories is a multimission laboratory managed and operated by National Technology and Engineering Solutions of Sandia, LLC, a wholly owned subsidiary of Honeywell International, Inc., for the U.S. Department of Energy's National Nuclear Security

Administration under contract DE-NA0003525. This paper describes objective technical results and analysis. Any subjective views or opinions that might be expressed in the paper do not necessarily represent the views of the U.S. Department of Energy or the United States Government.

VIII. Refences

[1] "Current Status of Depleted UF6." https://web.evs.anl.gov/uranium/guide/overview/uf6curr.cfm (accessed July 19, 2021).

[2] B. Marion. "Gamma Knife Surgery." http://large.stanford.edu/courses/2017/ph241/marion2/ (accessed July 19, 2021).

[3] "Americium-241/ Beryllium (AmBe) Sealed Sources for Industrial Process Control." https://raims.co.uk/product/americium-241-beryllium-ambe-sealed-sources-for-industrial-process-control/ (accessed July 19, 2021).

[4] S. Weinberger. "Nuclear Transport Trucks Revealed." https://www.wired.com/2009/09/nuclear-transport-trucks-revealed/ (accessed July 19, 2021).

[5] "Reflective Particle Tags (RPTs)," Image courtesy SNL ed.

[6] M. Arndt and L. Kiesewetter, "Coded labels with amorphous magnetoelastic resonators," *Magnetics, IEEE Transactions on,* vol. 38, no. 5, pp. 3374-3376, 2002, doi: 10.1109/tmag.2002.802287.

[7] C. Grimes *et al.*, "Wireless Magnetoelastic Resonance Sensors: A Critical Review," *Sensors,* vol. 2, no. 7, pp. 294-313, 2002. [Online]. Available: http://www.mdpi.com/1424-8220/2/7/294.

[8] K. F. Zeng, K. G. Ong, C. Mungle, and C. A. Grimes, "Time domain characterization of oscillating sensors: Application of frequency counting to resonance frequency determination," (in English), *Rev. Sci. Instrum.,* Article vol. 73, no. 12, pp. 4375-4380, Dec 2002, doi: 10.1063/1.1518128.

[9] R. O'Handley, *Modern Magnetic Materials: Principles and Applications*. Wiley-Interscience, 1999.

[10] C. A. Grimes, S. C. Roy, S. Rani, and Q. Cai, "Theory, instrumentation and applications of magnetoelastic resonance sensors: a review," (in Eng), *Sensors (Basel),* vol. 11, no. 3, pp. 2809-2844, 2011, doi: 10.3390/s110302809.

[11] J. F. Ziegler, *The stopping and range of ions in solids / J.F. Ziegler, J.P. Biersack, U. Littmark* (Stopping and ranges of ions in matter ; v. 1., no. Accessed from https://nla.gov.au/nla.cat-vn125402). New York: Pergamon, 1985.